

## **AqF026, a novel agonist of the water channel Aquaporin-1**

Andrea J Yool, Johann Morelle, Yvette Cnops, Jean-Marc Verbavatz, Ewan M Campbell,  
Elizabeth A.H. Beckett, Grant W Booker, Gary Flynn, and Olivier Devuyst

### **Supplemental Information and Data**

#### **Material and Methods**

**Supplementary Table 1:** Amino acid residues in the loop D domain implicated in the binding of AqF026 in AQP1, and equivalent residues in AQP4.

**Supplementary Table 2:** Primers used in real-time RT-PCR analyses.

**Supplementary Figure 1:** Effect of AqF026 on the expression of AQP1 in the peritoneal membrane.

**Supplementary Figure 2:** Chemical synthesis of AqF026.

## SI Materials and Methods

*In vitro assays:* Expression of human AQP1 or rat AQP4 in *Xenopus laevis* oocytes was done as described previously.<sup>1,2</sup> In brief, oocytes were removed from anaesthetised adult female *Xenopus laevis* by partial ovariectomy. Follicular coats were removed by collagenase digestion, and oocytes were maintained at 16-18 °C in isotonic ND96 saline supplemented with heat-inactivated horse serum (10%) for up to 3 weeks. 2-3 days prior to experiments, oocytes were injected with 1-2 ng of cRNA in 40 nl of sterile water for wild type AQP1 and AQP4, or 5-10 ng of cRNA in 40 nl of water for AQP1 mutant constructs. Amounts were adjusted empirically to account for differences between constructs and preparations of RNA in order to achieve similar levels of osmotic swelling, determined as oocyte lysis within 1-3 min of immersion in distilled water. cRNAs were synthesized in vitro (T3 polymerase mMessage mMachine kit; Ambion) from BamHI-linearised cDNA encoding human AQP1 (NM\_198098) and rat AQP4 (NM\_012825) provided by Prof. P. Agre (Johns Hopkins Bloomberg School of Public Health, Baltimore, MD), subcloned into the *Xenopus* expression vector (pXβGev). Site-directed mutations in AQP1 were generated by PCR using the QuikChange kit (Agilent Technologies, AU). Non-AQP1-expressing control oocytes without cRNA injection were prepared from the same batches of oocytes. Confocal images of permeabilized oocytes expressing AQP1 wild type or mutants were obtained after incubation with polyclonal rabbit antibodies direct against the carboxyl terminal domain of AQP1.<sup>1</sup> 1-2 h prior to quantitative swelling assays, oocytes were rinsed in standard Na<sup>+</sup> bath saline without serum or antibiotics. Na<sup>+</sup> bath saline contained 100 mM NaCl, 2 mM KCl, 4.5 mM MgCl<sub>2</sub>, and 5 mM HEPES, pH 7.3. AQP-mediated water permeability was measured as the rate of swelling in 50% hypotonic saline (Na<sup>+</sup> bath saline diluted with an equal volume of water). Swelling quantified by the relative increase in volume was measured from oocyte cross-sectional area by videomicroscopy (CCD camera; Cohu, San Diego, CA) using NIH ImageJ and Prism (GraphPad Software Inc., San Diego, CA) software. Data for oocyte volume (V) were standardised to the initial volume (V<sub>0</sub>), plotted as a function of time, and fit by linear regression. Swelling rates were determined as the slope values [(V/V<sub>0</sub>)\*10<sup>5</sup> \*s<sup>-1</sup>]. All animal procedures were approved by the University of Adelaide Animal Ethics committee and performed in accord with the Australian Code of Practice for the Care and Use of Animals for Scientific Purposes.

*AqF026 synthesis and application:* AqF026 was prepared efficiently via a two step process, in which furosemide was first converted to its methyl ester derivative; then alkylation of the

sulphonamide ester yielded AqF026 which was purified by column chromatography (Suppl. Fig. 2). For *in vitro* assays of swelling, AqF026 was dissolved in dimethylsulfoxide (DMSO) at 1000x stock concentrations, and diluted in standard isotonic Na<sup>+</sup> saline solution to yield the final concentrations indicated. Oocytes were incubated 2 to 3 h in isotonic Na<sup>+</sup> bath saline with AqF026 or DMSO vehicle prior to swelling assays. The effects of keeping the concentrations of DMSO constant were tested by adjusting stock solutions to provide a 0.1% DMSO vehicle concentration, showing no difference between this and the use of lower doses of DMSO or no DMSO at all. We previously showed that DMSO concentrations up to 100 fold higher than those used in these experiments had no effect on results of AQP-expressing oocyte swelling assays.<sup>3</sup> For *in vivo* studies, AqF026 was dissolved in DMSO at 100 mM, diluted 12 µl per ml in sterile 0.9% NaCl, and injected as a single bolus of 175 µl in the tail veins of mice at 30 min prior to the start of the experimental transport measurements. The estimated final systemic concentration of AqF026 was 15 µM assuming a total-body-water to body-weight ratio averaging 65% in adult mice.<sup>4</sup> Thus, the total body volume of water was calculated as 1 ml/g multiplied by 65% of the mouse body weight (g). Other concentrations were obtained by dilution in NaCl 0.9%. An equivalent volume of DMSO in sterile saline was injected for the vehicle control group (estimated <0.02% DMSO final systemic dose).

*Peritoneal transport studies and tissue sampling:* Transport of water and solutes across the peritoneal membrane was investigated in a mouse model of peritoneal dialysis using a 3.86% glucose-based dialysate (2.5 ml; DianealR, Baxter, Nivelles, Belgium) as described previously.<sup>5,6</sup> Blood and dialysate samples were taken at times 0, 30, 60, and 120 min of the dwell. Net ultrafiltration was measured at the end of the 120 min dwell. Instilled and recovered dialysate volumes were weighed on a precision balance (AG35, Mettler Toledo, Zaventem, Belgium; margin of error, 0.1 mg). Dialysate recovery was performed at the end of the dwell, using syringes and pre-weighed safe-lock tubes; the remaining dialysate in the peritoneal cavity was collected using gauze tissue, and weighed using the same technique. The fluid taken from gauze tissue accounted for ~5% of total volume of dialysate in both groups, in agreement with previous studies.<sup>5</sup> AqF026- and vehicle-treated mice had a similar dialysate volume recovered with the gauze tissue (209±15 µl versus 202±15 µl, respectively, *p*=0.74) and a standard deviation of 6% in both groups. Provided a 3.86% glucose dialysate density of 1.020 ± 0.001 g/cm<sup>3</sup> in experimental conditions, the volume margin of error can be calculated as 0.1 µl. Values rounded off to nearest µl were used for both instilled and

recovered volumes. This methodology has shown excellent reproducibility and the volume measurements have been validated independently by the three- pore model simulations.<sup>5,6</sup> The transport of small solutes was evaluated by the mass transfer area coefficient (MTAC) of urea, using the Waniewski equation ( $f=0.33$ ) to correct for convective processes,<sup>7</sup> and by the evolution over time of the dialysate-over-plasma concentration of urea (D/P urea) and the progressive removal of glucose standardised to the initial concentration in the dialysate (D/D<sub>0</sub> glucose). At the end of the dwell, mice were sacrificed by exsanguination and samples were processed for fixation and for mRNA and protein extractions.

*Intraperitoneal volume curves and calculation of initial ultrafiltration rates:* The peritoneal cavity of *Aqp1* wild-type and knock-out mice was infused with 2.5 ml of 3.86% glucose dialysate in which 100 µg of Alexafluor555-BSA (Molecular Probe, Eugene, OR) was added. Alexafluor555 is a bright, photostable and hydrophilic conjugate, which is covalently-bound to albumin and is well-suited for volume measurements in rodents.<sup>8</sup> Characterization of the tracer in the mouse model of PD revealed a minimal absorption in the plasma and peritoneal membrane during the dwell, as assessed by fluorescence spectrometry (LS55, Perkin-Elmer, Waltham, MA) and high-performance liquid chromatography (C4 Vydac column, Dionex capillary HPLC, Dionex Benelux, Amsterdam, The Netherlands) using standards to prevent quenching and non-specific interference after extraction.<sup>8</sup> Both techniques failed to detect significant traces of Alexafluor555-BSA in plasma and peritoneal membrane (detection limit ~1µg/ml, i.e. <3% of the dose injected), confirming the high intraperitoneal recovery of this tracer. Further validation of Alexafluor555-BSA for intraperitoneal volume (IPV) measurement included comparison with volumetric assessment (gold-standard) at different time points and demonstration of the known influence of AQP1 on the IPV curves and derived initial UF rates obtained in *Aqp1* mice using RISA.<sup>6</sup>

The specific properties (negative charge, hydrophilicity) of Alexafluor555, which is obtained by sulfonation of rhodamine, and its stable covalent binding to albumin, which contrasts with the notoriously unstable RISA used in most peritoneal studies, are probably responsible for the surprisingly high recovery of the tracer in this model.

For IPV measurements, dialysate was microsampled at 0, 10, 30, 60, 90 and 120 min of the dwell and fluorescent intensity was assessed using a LS55 fluorescence spectrometer.

Intraperitoneal fluorescent albumin concentration was obtained from the linear relationship between relative fluorescence intensity and Alexafluor555-BSA concentration. The intra-peritoneal mass of Alexafluor555-BSA remained almost constant during the dwell (relative

albumin mass at 120min  $0.99 \pm 0.03$ ). Intraperitoneal volume at time  $t$  ( $V_t$ ) was thus calculated using the following equation:

$$V_t = \frac{C_0 \times V_{in}}{C_t}$$

in which  $V_{in}$  is the instilled dialysate volume,  $C_0$  and  $C_t$ , the intraperitoneal fluorescent albumin concentrations at 0 min and at time  $t$ , respectively. Initial UF rate was derived from intraperitoneal volume versus time curve. Equivalent procedures were applied to obtain the IPV in the *Aqp1* wild-type and knock-out mice.

*Transmission electron microscopy:* Mouse peritoneum was processed for ultrastructural studies and immunogold labelling as previously reported.<sup>5</sup> For immunogold labeling, peritoneum samples (7 controls injected with DMSO alone and 7 treated with AqF026) were fixed in 4% paraformaldehyde in PBS, dehydrated in graded ethanol concentrations and embedded in LR-White resin. Sections (70 nm-thick) were incubated with the primary antibody (rabbit anti-AQP1, 3 mg/ml final concentration) and after washing, with a 1:60 dilution of 10nm protein-A gold anti-rabbit antibody, washed again and stained in 2% uranyl acetate in water followed by lead citrate. The sections were observed on a Tecnai-12 microscope (FEI, Eindhoven) and photographed at x11000 magnification at a resolution of 1.2 nm/pixel. A total of 26 capillaries were imaged from each sample. The number of particles per unit length of capillary was measured using the IMOD software.<sup>9</sup> In sum, results were calculated from >9000 particles over >1500  $\mu\text{m}$  capillary length in each experimental condition.

## References

1. Anthony TL, et al. Cloned human aquaporin-1 is a cyclic GMP-gated ion channel. *Mol Pharmacol* 57: 576-588, 2000
2. Campbell EM, Birdsell DN, Yool AJ. The Activity of Human Aquaporin 1 as a cGMP-gated Cation Channel is Regulated by Tyrosine Phosphorylation in the Carboxyl Terminal Domain. *Mol Pharmacol* 81: 1-9, 2012
3. Migliati E, et al. Inhibition of aquaporin-1 and aquaporin-4 water permeability by a derivative of the loop diuretic bumetanide acting at an internal pore-occluding binding site. *Mol Pharmacol* 76: 105-112, 2009
4. Chapman ME, Hu L, Plato CF, Kohan DE. Bioimpedance spectroscopy for the estimation of body fluid volumes in mice. *Am J Physiol Renal Physiol* 299: F280-F283, 2010
5. Ni J, et al. Functional and molecular characterization of a peritoneal dialysis model in the C57BL/6J mouse. *Kidney Int* 67: 2021-2031, 2005
6. Ni J, et al. Aquaporin-1 plays an essential role in water permeability and ultrafiltration during peritoneal dialysis. *Kidney Int* 69: 1518-1525, 2006

7. Waniewski J, et al. Simple models for description of small-solute transport in peritoneal dialysis. *Blood Purif* 9: 129-141, 1991
8. Curry FR, et al. Atrial natriuretic peptide modulation of albumin clearance and contrast agent permeability in mouse skeletal muscle and skin: role in regulation of plasma volume. *J Physiol* 588: 325-339, 2010
9. Kremer JR, Mastronarde DN, McIntosh JR. Computer visualization of three-dimensional image data using IMOD. *J Struct Biol* 116: 71-76, 1996

**Supplementary Table 1.** Amino acid residues in the loop D domain implicated in the binding of AqF026 in AQP1, and equivalent residues in AQP4.

<b><u>Human AQP1</u></b>	<b><u>Bovine AQP1</u></b>	<b><u>Rat AQP4</u></b>
Ala 64	Ala 66	Val 85
Thr 156	Thr 158	Ser 177
<b>Thr 157</b>	<b>Thr 159</b>	<b>Cys 178 *</b>
<b>Arg 159</b>	<b>Arg 161</b>	<b>Ser 180 **</b>
Asp 163	Asp 165	Asp 184
Leu 164	Leu 166	Val 185
Pro 169	Pro 171	Ala 190
Ile 172	Ile 174	Ile 193

\* block by internal mercuric compound in AQP4

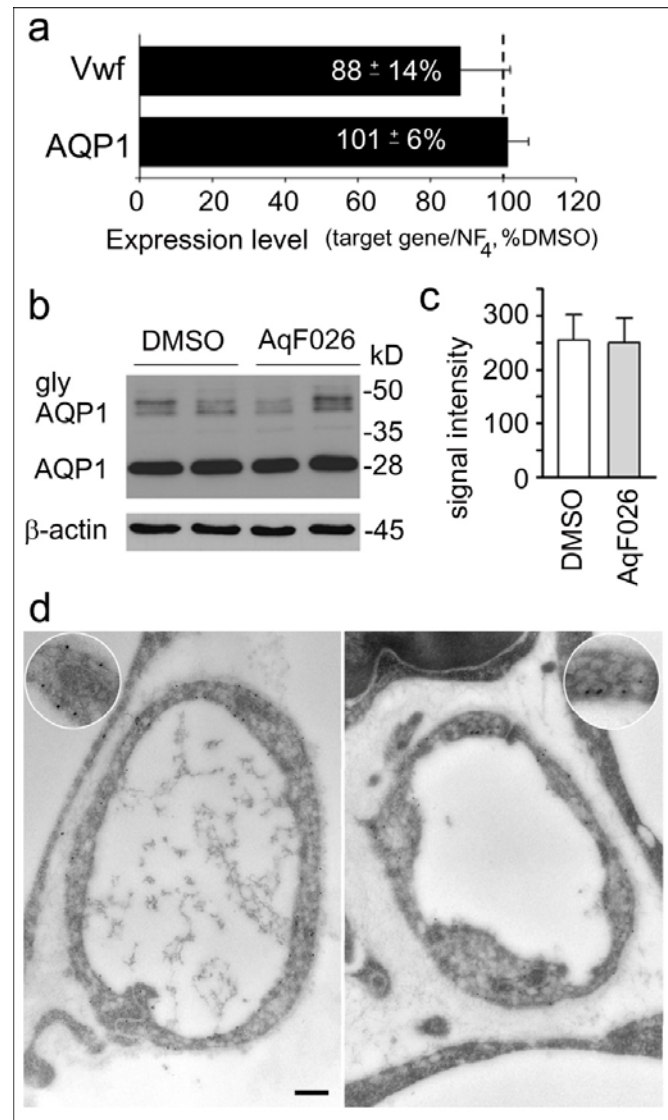
\*\* inhibition by phosphorylation in AQP4

**Supplementary Table 2.** Primers used in real-time RT-PCR analyses.

<u>Gene</u>	<u>Forward primer (5'-3')</u>	<u>Reverse primer (5'-3')</u>	<u>PCR Product (bp)</u>	<u>Efficiency</u>
<i>Actb</i>	TGC CCA TCT ATG AGG GCT AC	CCC GTT CAG TCA GGA TCT TC	102	1.02 ± 0.02
<i>Gapdh</i>	TGC ACC ACC AAC TGC TTA GC	GGA TGC AGG GAT GGG GGA GA	176	1.04 ± 0.03
<i>Arbp</i>	CTT CAT TGT GGG AGC AGA CA	TTC TCC AGA GCT GGG TTG TT	150	0.99 ± 0.01
<i>Ppia</i>	CGT CTC CTT CGA GCT GTT TG	CCA CCC TGG CAC ATG AAT C	139	1.02 ± 0.02
<i>Hprt1</i>	ACA TTG TGG CCC TCT GTG TG	TTA TGT CCC CCG TTG ACT GA	162	0.99 ± 0.01
<i>Aqp1</i>	GCT GTC ATG TAC ATC ATC GCC CAG	AGG TCA TTG CGG CCA AGT GAA T	107	0.99 ± 0.02
<i>Vwf</i>	CCC TCT CTC AGG ACT GCA AC	ATT GGC AGA TCC CAC TGA AG	150	0.98 ± 0.03

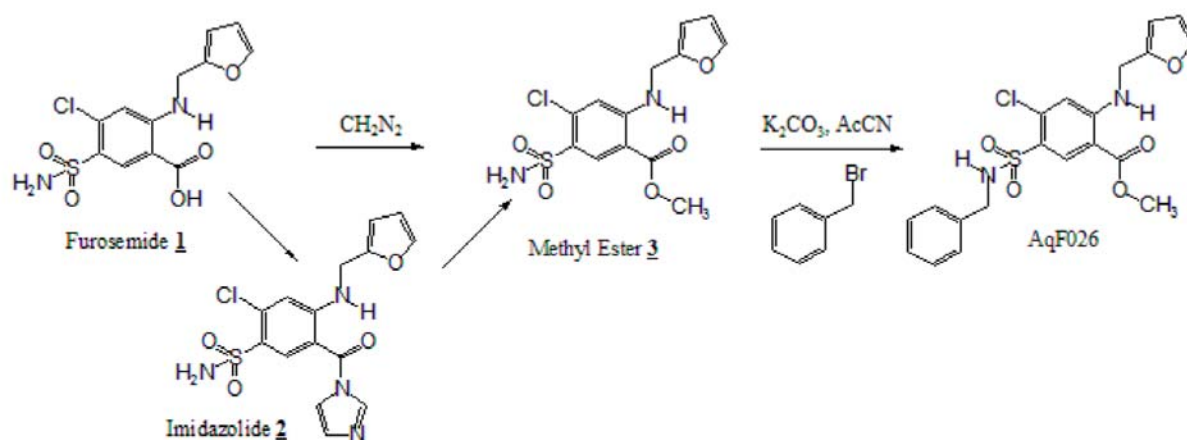
The primers were designed using Beacon Design 2.0 (Premier Biosoft International, Palo Alto, CA).

**Supplementary Figure 1.** Effect of AqF026 on the expression of AQP1 in the peritoneal membrane.



**(a)** Real-time RT-PCR quantification for mRNA expression of aquaporin-1 (AQP1) and von Willebrand factor (Vwf) in the mouse peritoneum. Treatment with AqF026 did not induce significant changes in the expression of either endothelial marker. **(b)** Representative immunoblots for AQP1 (1:20,000) in peritoneum extracts prepared from *Aqp1*<sup>+/+</sup> mice (20 µg protein/lane). The blots were stripped and reprobed with a monoclonal antibody against beta-actin (1:10,000) as a loading standard for accuracy. The core (28 kD) and glycosylated (35-50 kD) AQP1 isoforms were identified in the peritoneum, with no changes observed in the agonist- or DMSO vehicle-treated mice. **(c)** Densitometric analysis of AQP1 signal on 4 pairs of peritoneal samples. **(d)** Representative micrographs of immunogold labeling for AQP1 in control (left) and treated (right) samples. Gold particles decorated the endothelial cells of blood capillaries and exhibited no change in localization after treatment. Insets: x2 magnification. Bar = 250 nm.

**Supplementary Figure 2.** Chemical synthesis of AqF026.



Furosemide (**1**) was converted to its methyl ester derivative (AqF022) (**3**) by monitoring the addition of diazomethane until only a slight yellow tint remained. Prolonged treatment with excess diazomethane was found to result in varying degrees of sulphonamide methylation. Alternatively, furosemide was specifically converted by carbonyl diimidazole to its imidazolidine derivative (**2**) which cleanly provided methyl ester (**3**) upon addition of methyl alcohol. Alkylation of sulphonamide ester (**3**) with benzyl bromide and potassium carbonate in acetonitrile afforded AqF026 after purification by column chromatography.